A Weibull Approach for Recalibrating Climate Model Projections of Tropical Cyclone Wind-speed Distributions

Mari R. Jones Tye[1*], David B. Stephenson[2], Greg J. Holland[1], Richard W. Katz[1]

1 National Center for Atmospheric Research, P.O. Box 3000, Boulder, CO, 80307

2 Exeter Climate Systems, Mathematics Research Institute, University of Exeter, Exeter, U.K.

Abstract

Reliable estimates of future changes in extreme weather phenomena, such as tropical cyclone maximum wind speeds, are critical for climate change impact assessments and the development of appropriate adaptation strategies. However, Global and Regional Climate Model outputs are often too coarse for direct use in these applications, with variables such as wind speed having truncated probability distributions compared to those of observations. This poses two problems: how can we best adjust model-simulated variables to make them more realistic; and how can we use such adjustments to make more reliable predictions of future changes in their distribution.

This study investigates North Atlantic tropical cyclone maximum wind speeds from observations (1950-2010) and Regional climate model simulations (1995-2005 and 2045-2055 at 12km and 36km spatial resolutions). The wind speed distributions in these datasets are well represented by the Weibull distribution, albeit with different scale and shape parameters.

A power law transfer function is used to recalibrate the Weibull variables and obtain future projections of wind speeds. Two different strategies, bias correction and change factor, are tested by using 36km model data to predict future 12km model data (pseudo-observations). The strategies are also applied to the observations to obtain likely predictions of the future distributions of wind speeds. The strategies yield similar predictions of likely changes in the fraction of events within Saffir-Simpson categories e.g. an increase from 21% (1995-2005) to 27-37% (2045-55) for CAT3 or above events and an increase from 1.6% (1995-2005) to 2.8-9.8% (2045-55) for CAT5 events.

1 Introduction

Reliable estimates of future changes in extreme weather phenomena, such as tropical cyclone (TC) maximum wind speeds (v_{max}), are critical for climate change impact assessments and the development of appropriate adaptation strategies. With increases in the most intense tropical cyclones in the Western North Pacific and North Atlantic *more likely than not* over coming decades (IPCC 2013), identifying the likely future range of TC maximum wind speeds is essential. However, climate models are unable to resolve fully all the processes within tropical cyclones, resulting in simulated maximum wind speeds with very different probability distributions from those of observed wind speeds. While the realism of maximum wind speeds improves with increases in model resolution (Done et al. 2013; Bender et al. 2010), or by running high resolution coupled simulations along synthetic cyclone tracks (e.g. Emanuel 2006), such simulations are computationally expensive and consequently not available to many decision makers. While some high grid resolution climate change projections have been used for assessments (e.g. Murphy et al. 2009; Whetton et al. 2012), most adaptation and mitigation decisions (e.g. Executive Office of the President 2013; Benton et al. 2012) are informed by lower resolution global models (Brown and Wilby 2012) such as those involved in the CMIP5 (Climate Model Intercomparison Project) experiment (Knutti et al. 2013).

Many statistical downscaling techniques exist, each with benefits and disadvantages relative to the application in question (e.g. refer to Maraun et al. 2010; or Rummukainen 2010 for recent summaries). However, downscaling techniques that are

effective for daily temperature or precipitation may not be appropriate for extreme wind speeds (Curry et al. 2011). Some statistical downscaling methods attempt to relate the probability density functions (PDFs) of model simulated and observed data through a transfer function (e.g. Piani et al. 2009). This transfer function may represent a relationship with larger scale atmospheric variables (Salameh et al. 2008; van der Kamp et al. 2011; Kallache et al. 2011) or a transfer through a distribution such as the exponential (Piani et al. 2009). However, it is important to note that the transformations are sensitive both to the selected calibration method and to the "calibration pathway" from observations to the estimated future output (Ho et al. 2012).

This study fits Weibull distributions to observed and model-simulated tropical cyclone maximum wind speeds and assesses the goodness of fit. The Weibull distribution is used to develop an appropriate power law transfer function for mapping between model wind speeds and observed wind speeds. Unlike quantile-quantile matching, this parametric approach can be used to map values greater than those observed historically. Model-simulated wind velocity components are used to diagnose why model simulated and observed wind speeds have distributions with such different Weibull shapes. The power law transfer function is used to make projections of future wind speeds using both the bias correction and the change factor strategies. The approaches are then tested by treating the higher-resolution 12km data as pseudo-observations.

The data used in this research are described in Section 2 and the underlying statistical methods are outlined in Section 3. Section 4 presents initial analyses of the wind speed components, while Section 5 presents the anticipated changes in the distribution of future maximum wind speeds.

2 Data

Observations are taken from the historical archive of North Atlantic tropical cyclones from the IBTrACS database (Knapp et al. 2010), with intensities corrected for high biases arising from early aircraft reconnaissance as in Holland (2008). The series extends from 1950-2010, recorded in discrete 5-knot intervals; a uniform distribution "jitter" on the interval (-2.5, 2.5) has been added to the wind speeds prior to analysis to alleviate the artificial discretization.

Modeled data utilize the NCAR archive of Nested Regional Climate Model (NRCM) simulations for the periods 1990-2005 and 2045-2055 (Done et al. 2013). The NRCM simulations are derived from a 36km grid using the Weather Research and Forecasting (WRF) model (Skamarock et al. 2008) nested one-way within the 2.5°x2.5° Community Climate System Model version 3 (CCSM3, Collins et al. 2006) run in "climate" mode from 1950 using the A2 emissions scenario (IPCC SRES SPM 2000). Higher resolution simulations are derived from a further one-way nest of the 12km grid WRF model run in "climate" mode within the 36km model output. For clarity, IBTrACS wind speeds are referred to as *observed* and NRCM model wind speeds are referred to as *simulated*.

Figure 1 compares the observed, and 36km and 12km simulated TC v_{max} relative frequency distributions and highlights the tendency of models to underestimate the most intense tropical cyclones and overestimate moderate intensity systems (Done et al. 2013); observed TC v_{max} are also lower-truncated. Model simulations of the 36km (1c,d) and 12km (1e,f) differ considerably in shape and skewness from the observed distribution (1a); 1(b) highlights the absence of realistic future estimates of maximum wind speeds.

Maximum sustained winds reported in the IBTRACs database are the 10 minute average maximum intensity at 10m above the sea surface and may contain some sub-tropical systems; moreover, historical wind speeds were subjectively reported and less reliable at low intensities (Kossin et al. 2007). For consistency with the tracking algorithm used to identify simulated tropical cyclones (Suzuki-Parker 2012), observed TC v_{max} are assumed to be truncated at $17ms^{-1}$. Davis *et al.* (2008) demonstrated that model resolutions approaching 1km are needed to reproduce the full range of observed maximum wind speeds.

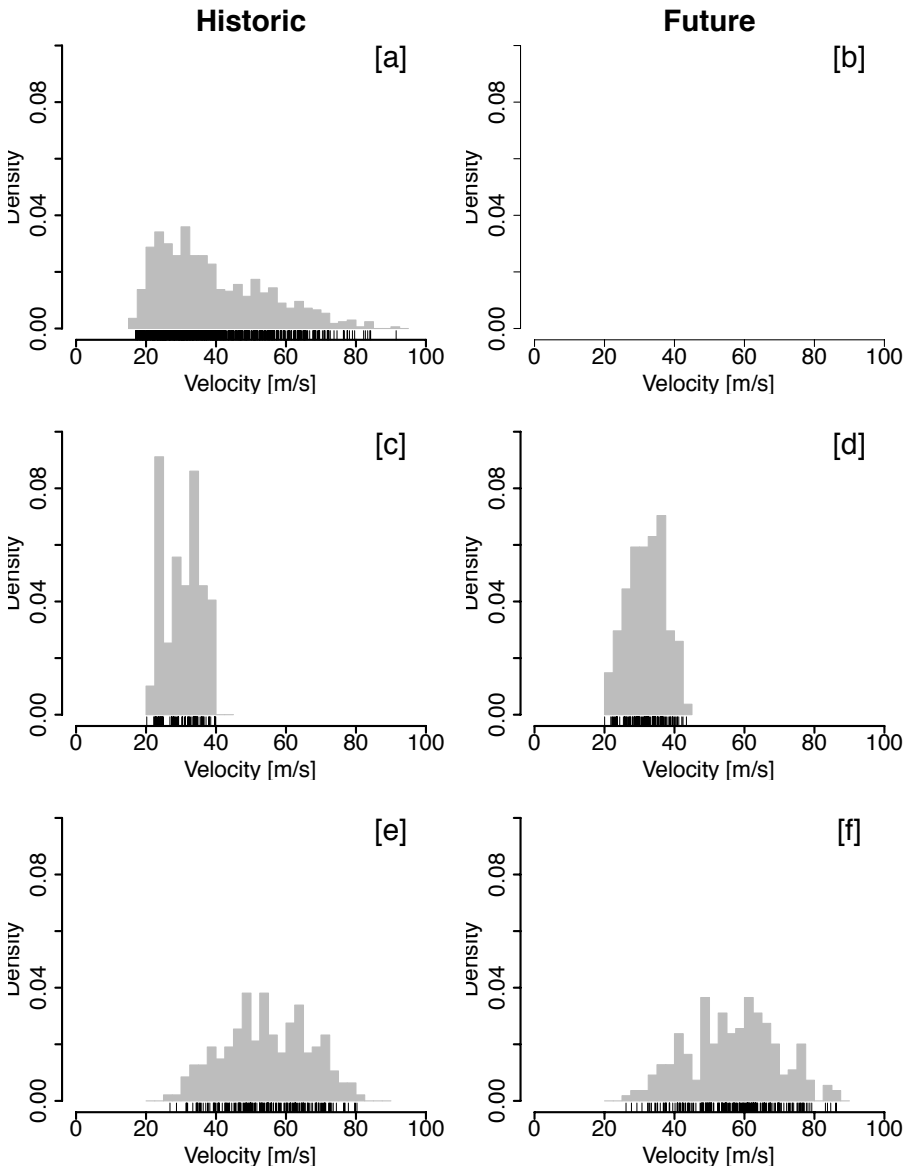

Figure 1 : Relative frequency of observed and model simulated TC maximum wind speeds. (a) Observations 1950-2010; (b) Future observations; (c) 36km Simulations 1995-2005; (d) 36km Simulations 2045-2055; (e) 12km Simulations 1995-2005; and (f) 12km Simulations 2045-2055. The distributions have notably different scale and shape. Note the difference in the highest maximum speed on the abscissa.

3 Methods

3.1 Weibull Distribution

The two-parameter Weibull distribution (Weibull 1939; Stewart and Essenwanger 1978) has long been established as a useful probability distribution for representing wind speeds (Justus et al. 1978; Conradsen et al. 1984). The Weibull distribution, with scale parameter $\alpha > 0$ and shape parameter $\beta > 0$ has cumulative distribution function for x>0 given by

$$\Pr(X \le x) = F(x;\alpha,\beta) = 1 - \exp\left(-\left(\frac{x}{\alpha}\right)^{\beta}\right) \quad (1)$$

The special case of the Weibull distribution with shape parameter equal to 2 (the Rayleigh distribution) occurs if the wind velocity (u,v) components are independent and identically Normally distributed (Tuller and Brett 1985). Zhou & Smith (2013) identified considerable regional variability in the shape parameter, with values ranging from 1 to 4; however, they suggest that a comparison of Weibull distribution parameters may provide a useful way to capture differences between observed and simulated wind speeds. The independent and identically Normally distributed relationship that has been exploited by others to improve statistical downscaling (Monahan 2011), particularly in areas of high topography (Salameh et al. 2008). Pryor (2005) found, in common with others (Tuller and Brett 1985; Salameh et al. 2008), that the Weibull distribution does not provide a good fit to high wind speeds where there is variable topography or synoptic flow forcing, and tends to overestimate the highest maximum values (Jagger et al. 2001). Since the Weibull distribution is unbounded above it will overestimate the probability of wind speeds above the physical upper limit (Holland and Bruyère 2014). However, when an

allowance is made for observed and modeled truncation at low wind speeds, the Weibull distribution represents model and observed wind speeds sufficiently to enable statistical downscaling (Curry et al. 2011; Pryor and Barthelmie 2013).

Batts & Simiu (1980) identified that observed and modeled tropical cyclone maximum wind speeds were best represented by a Weibull distribution for probability estimates. More recently, Jagger et al. (2001) extended the Weibull distribution with linear regression models to represent spatial and temporal variations in the distribution parameters, concluding that this is an effective representation of the dynamic probability. Others have explored changes in tropical cyclone maximum wind speed using the Generalized Extreme Value (GEV) distribution for both the maximum over several storms (e.g. Heckert et al. 1998) or the maximum over the life of the storm (e.g. Bürger et al. 2012). However, we consider that the GEV is not appropriate for this application with tropical cyclone maximum wind speeds over individual storms as the observations at different grid points are strongly dependent, contravening the assumption that data are the maxima of independent or only weakly dependent variables.

3.1.1 Estimation of the Weibull parameters

The wind speeds used for our analyses are for features identified with at least tropical storm status on the Saffir-Simpson scale (Simpson and Riehl 1981), so very low wind speed values below u=17ms^{-1} are not included. In other words, our data are left-truncated with wind speeds only above u and so should be fitted to the left-truncated Weibull distribution having cumulative distribution function

$$\frac{F(x;\alpha,\beta)-F(u;\alpha,\beta)}{1-F(u;\alpha,\beta)} \quad (2)$$

where F is given by Equation (1). Failure to acknowledge such truncation in the wind speeds leads to biases in the Weibull parameter estimates. Table 1 gives the scale and shape parameter estimates found using Maximum Likelihood Estimation (see R code in Appendix 1) assuming a truncation threshold of u=17ms^{-1}; error estimates were obtained from the variance-covariance matrix of 100 bootstrapped samples. The shape parameter estimates are very different for observed and model-simulated wind speeds. The shape parameter estimate for the observed wind speeds is close to the value of 2 (Rayleigh distribution) whereas the model-simulated wind speeds have shape parameters greater than 4 (much more peaked distributions). The reasons for this are diagnosed in the next section. Table 1 also contains summary statistics for each of the data sets, indicating that the different shape and scale are not due solely to finite sampling over short model time periods.

Table 1 : Summary statistics and Weibull parameter estimates (standard errors) for observed and model maximum wind speeds

	Sample size	Mean (ms^{-1})	Minimum (ms^{-1})	Maximum (ms^{-1})	Scale (α ms^{-1})	Shape (β)
1950-2010 Observations	668	39.04	17.00	91.48	39.16 (1.05)	2.09 (0.01)
1995-2005 Observations	168	39.06	17.00	81.53	37.40 (7.46)	1.85 (0.03)
1995-2005 36km Model	79	30.52	20.21	39.93	32.23 (0.81)	5.91 (0.42)
2045-2055 36km Model	108	32.07	20.04	43.41	34.05 (0.34)	6.43 (0.28)
1995-2005 12km Model	189	54.49	28.70	80.29	58.89 (1.28)	4.85 (0.07)
2045-2055 12km Model	219	56.56	27.70	86.22	61.26 (0.82)	4.83 (0.06)

The goodness of fit can be assessed by plotting quantiles from the fitted Weibull distributions against the empirical quantiles in each data set (Figure 2). The line $y=x$ generally lies well within the 95% confidence intervals on the quantile-quantile plots for all data sets, indicating that the fitted Weibull distributions well represent the empirical distributions. The 95% confidence intervals (in grey) were estimated from randomly sampling 1000 times from each fitted distribution. There is evidence of a slight positive curvature at very high wind speeds, which is most likely related to the unbounded nature of the Weibull distribution. The tail of the fitted Weibull is too heavy for the most intense observed wind speeds (e.g. Wilks 2011 p115).

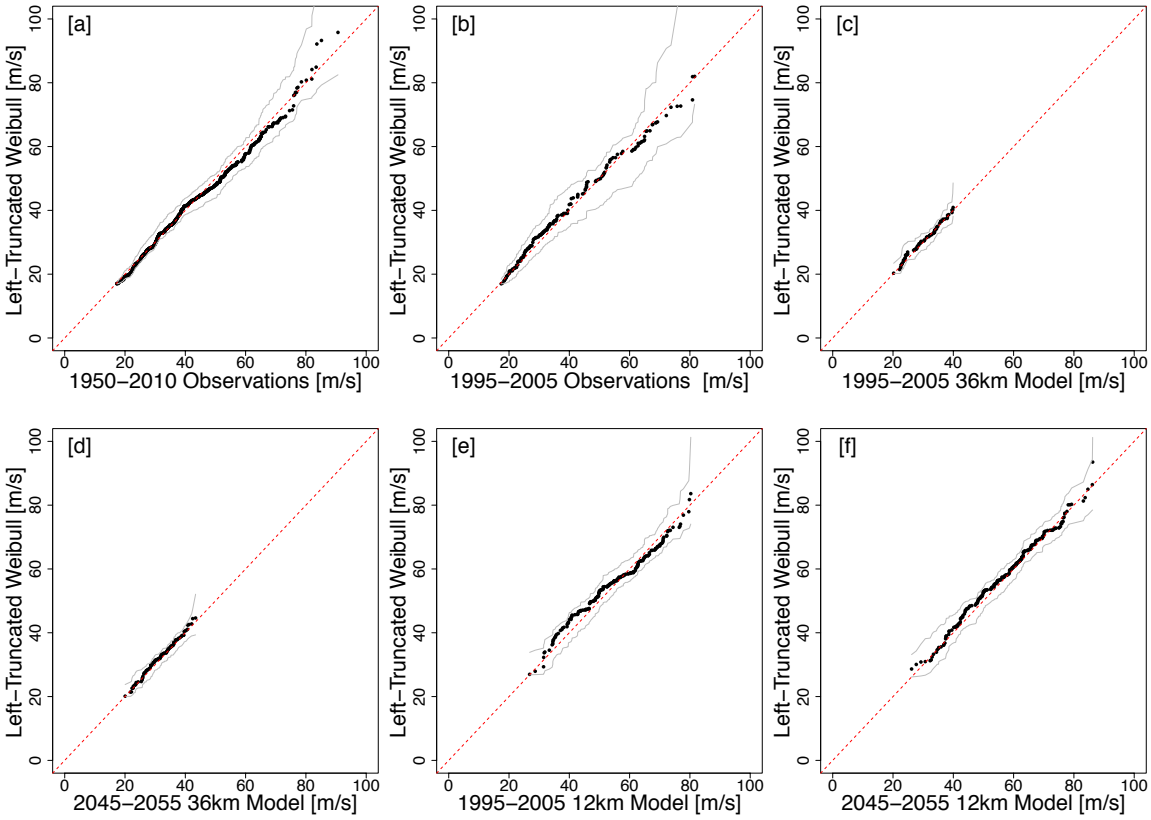

Figure 2 : Goodness of fit of two-parameter Weibull distributions. Plots show quantiles of the wind speeds vs. quantiles from the fitted distributions for (a) observed (1950-2010); (b) observed (1995=2005); (c) 36km model simulated control period (1995-2005); (d) 36km future period (2045-2055); (e) 12km model simulated control period (1995-2005); and (f) 12km future period (2045-2055) maximum wind speeds.

3.2 Why are the distribution shapes so different?

If the orthogonal velocity components (u,v) are independent with zero mean and equal variance and are approximately Normally distributed, the wind speed can be shown mathematically to be Weibull distributed with shape parameter equal to 2 (Monahan 2011; Tuller and Brett 1985). While these assumptions cannot be tested for this set of observed maximum wind speeds, as the vector components are not available, it is possible to examine whether the model shape parameters differ from 2 because one of these assumptions is violated. Each assumption required to satisfy the Rayleigh

distribution has been tested here for the control period (1995-2005) of the 36km simulation.

3.2.1 Zero mean

Sample means from the 36km model simulated maximum wind speeds were removed from the u and v components separately before recalculating the distribution parameters. This had the effect of reducing the shape parameter to 3.11 for the model wind speeds from 5.91. If the variance in the components were higher, the effect of non-zero means would have had a smaller relative contribution on the reduction in the shape parameter.

3.2.2 Equal variance

A further re-scaling of the u and v components by their respective standard deviations had little impact on the parameter estimates, achieving a reduced shape parameter of 3.08. As the u and v components had similar standard deviations with 19.69 and 20.15, respectively, the minimal improvement beyond that achieved by centering the data was unsurprising.

3.2.3 Normal distribution

A qualitative way to assess how far the velocity components differ from the Normal is through comparison of scatter plots of the model u and v components to simulations of normal velocity components that are truncated above the minimum observed wind speed (Figure 3). The u and v velocity components appear to be less spread than simulated Normally distributed components, that is they have shorter tails than Normal (platykurtic).

3.2.4 Independence

The estimated correlation between the u and v components for the model wind speeds is very small at 0.0012; this is unlikely to be the reason why the model speeds are not Rayleigh distributed. No obvious non-linear dependence can be seen in scatter plots of the u and v components (Figure 3a). It is reasonable to assume that the model velocity components are independent of each other because tropical cyclones propagate and rotate rather than remaining static, which helps remove dependence between the parameters (Monahan 2013).

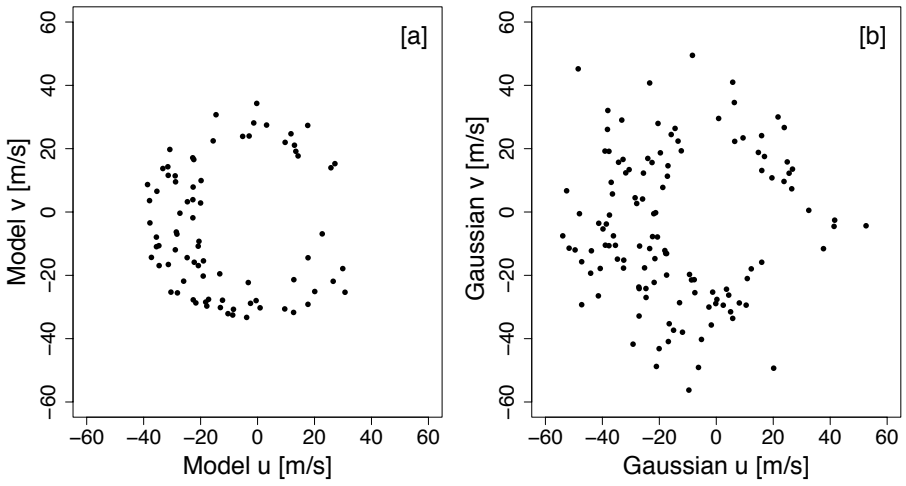

Figure 3 : Scatter plots of u and v velocity components for (a) model simulated maximum wind speeds; and (b) simulated from independent Gaussian distributions truncated to match the minimum model wind speed (20.21 ms^{-1}). Note the increased scatter of points further away from the origin in the Gaussian simulation.

To test whether the combined influence of these adjustments would bring model wind speeds closer to observed maximum wind speeds, Normal variates were added to each velocity component. That is, u and v components were adjusted for zero mean and standard deviations (of around 20ms^{-1}) increased by 3.79ms^{-1} to derive a mean of the squared adjusted wind speed components equal to the square of the observed wind

speeds. This reduced the shape parameter estimate to 2.09, equal to the shape of the distribution of the observed wind speeds.

It appears that the lack of variance in the model velocity components is the main cause of the wind speed distributions being more peaked and having a larger Weibull shape parameter. The model velocity components are more constrained (platykurtic) than Normally distributed variables, accounting for the remainder of the difference between the distribution shape parameters. Platykurtic velocity components indicate the inability in the model to simulate extremes in the velocity components arising from the low resolution of the models with respect to the scale of the observed physical processes required for tropical cyclone growth (Done et al. 2013).

3.3 Transforming variables to have different Weibull distributions

When two variables, such as observed and model-simulated wind speeds, come from the same family of distributions, then the common form of the distribution provides a simple way of mapping one variable to have the same distribution as the other (e.g. Piani et al. 2009 for mapping between Gamma distributed variables). It can be shown that if random variable X is Weibull distributed with scale parameter, α, and shape parameter, β, then $Z = \left(X / \alpha \right)^{\beta}$ will be exponentially distributed. Hence, X can be transformed into a Weibull variable X^* having scale and shape parameters, α^* and β^*, by the following power law transfer function:

$$X^* = \alpha^* \left(\frac{X}{\alpha} \right)^{\beta/\beta^*} \tag{3}$$

Taking the logarithms of both sides of Equation 3, reveals that the log-transformed Weibull variables are linearly related to one another by:

$$\log X^* = \log \alpha^* - \frac{\beta}{\beta^*} \log \alpha + \frac{\beta}{\beta^*} \log X$$

Since the transfer function is monotone, this relationship is also shared by the quantiles of the log-transformed variables (Stewart and Essenwanger 1978). The validity of this relationship can be tested by making quantile-quantile plots of the log-transformed variable. Figure 4 shows quantile-quantile plots for the logarithm of the wind speeds between observations (1950-2010) and the simulations. There is a reasonable linear relationship between all of the data sets, which justifies our later use of this power law transform to recalibrate the wind speeds.

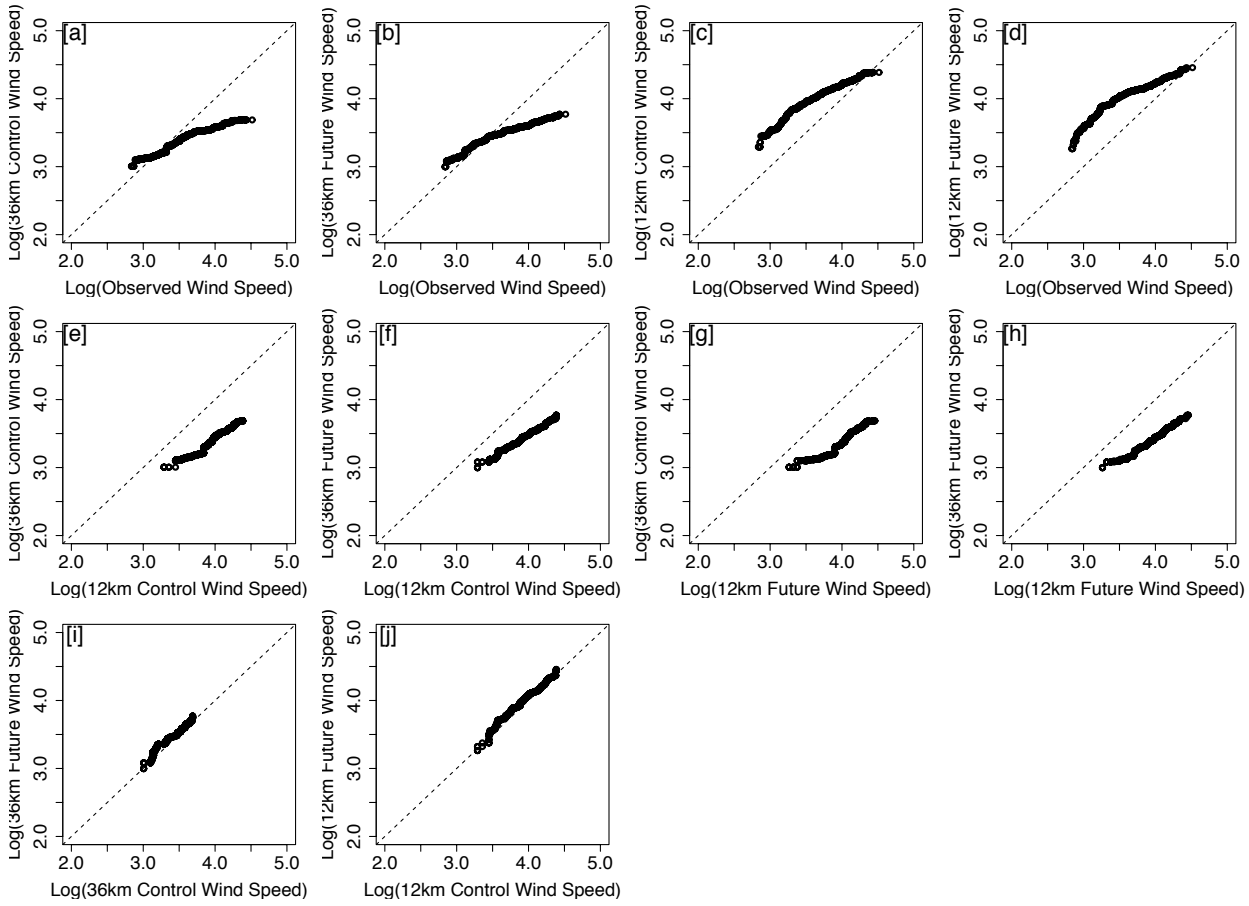

Figure 4 : Quantile-quantile plots of log wind speed illustrating linear relationship between (a) observations and 36km control simulations; (b) observations and 36km future simulations; (c) observations and 12km control simulations; (d) observations and 12km future simulations; (e) 12km and 36km control simulations; (f) 12km control and 36km future simulations; (g) 12km future and 36km control simulations; (h) 12km and 36km future simulations; (i) 36km control and future simulations; and (j) 12km control and future simulations. Distributions are identical if points lie on the line *y=x* (dashed line).

4 Recalibration of Model Maximum Wind Speeds

4.1 Calibration pathways

Two calibration pathways can be considered when downscaling model-simulated projections to obtain a more realistic future: bias correction (BC) and change factor (CF). The first assumes that differences between the control model (M_c) and current

observations (O_c) remain the same in the future (O_f) (*Change Factor*); pathway 1 in Figure 5. The second pathway assumes that the difference between the control (M_c) and future (M_p) model outputs is the same as for observed and projected data (*Bias Correction)*; pathway 2 in Figure 5. Ho et al. (2012) demonstrated that these two calibration pathways give very different estimates of future daily surface air temperature. Intuitively this result is obvious when applied to the distribution of wind speeds as the differences in variance are treated in different ways, and yet estimates of future impacts often employ only one recalibration method (e.g. Piani et al. 2009; Lafon et al. 2013).

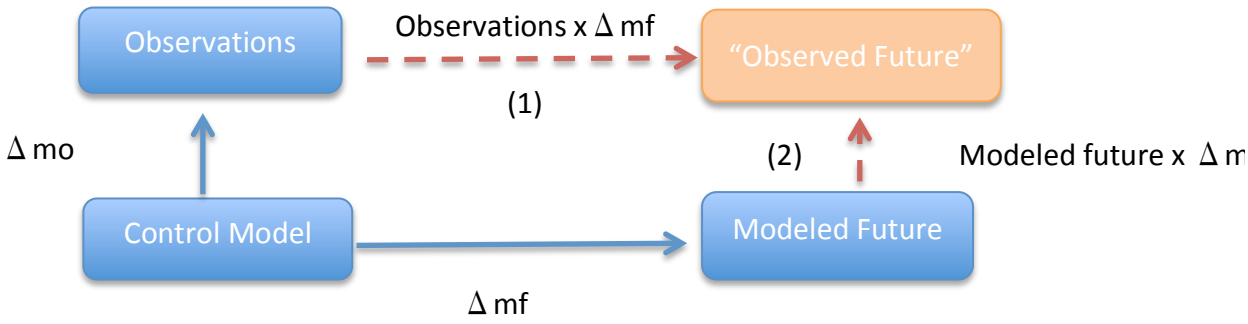

Figure 5 : Calibration pathways: (1) Change Factor and (2) Bias Correction

New estimates of the transformed shape, β, and scale, α, parameters are derived below for each calibration pathway; derivations of the transformations are included in Appendix 2. The "future observed" shape parameter is the same for both calibration pathways and derived as follows:

$$\beta_{o'} = \frac{\beta_o \beta_{mf}}{\beta_m} \tag{4}$$

The bias corrected scale parameter is defined in terms of the ratio of the scale parameters between the future and control simulations and also depends on the ratio of shape parameters:

$$\alpha_{o'BC} = \alpha_o \left(\frac{\alpha_{mf}}{\alpha_m} \right)^{\beta_m/\beta_o} \tag{5}$$

while the change factor correction to the scale parameter is defined in terms of the ratio of the control simulation and the observations scale parameters:

$$\alpha_{o'CF} = \alpha_{mf} \left(\frac{\alpha_o}{\alpha_m} \right)^{\beta_m/\beta_f} \tag{6}$$

Note that Equations (5) and (6) will differ unless all three shape parameters (beta_o, beta_m, beta_mf) are identical.

4.2 Method Validation

To assess the performance of the recalibration methods, a proxy experiment was carried out using the higher resolution grid model outputs. As the 36km and 12km model simulated wind speeds have a similar range and maximum/minimum values, this experiment is not a true test of the adequacy of the method to downscale to reality. However, it may remove some ambiguity from selecting the most appropriate calibration pathway.

The 12km model simulated wind speeds are treated as pseudo-observations and their future distribution is predicted using the 36km wind speed data. The recalibrated "future" parameters were then compared to the Weibull parameters for the 12km future

model (Figure 6). The 95% confidence interval was established from the variance-covariance matrix of Weibull parameter estimates from 100 bootstrapped samples.

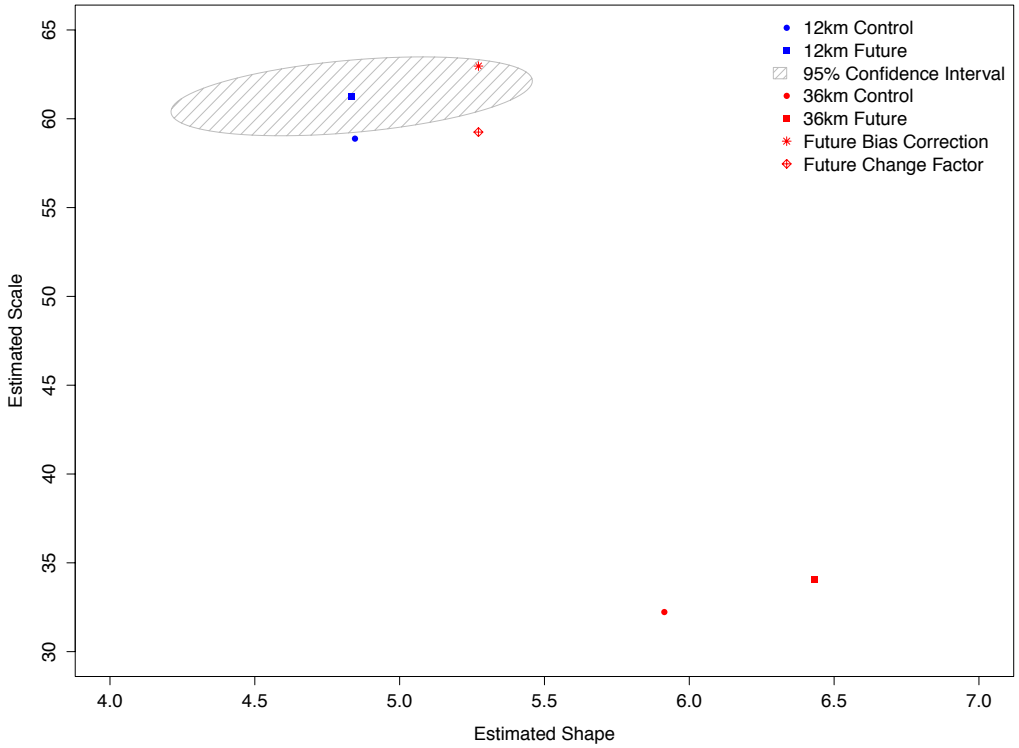

Figure 6 : Assessment of calibration pathways from the 36km model to obtain the 12km future estimates. Filled circles represent fitted control model parameters; squares represent fitted future model parameters; filled rectangle indicates parameter estimates confidence interval for the fitted 12km future distribution.

Neither calibration pathway is correct, with Bias Correction overestimating, and Change Factor underestimating, the scale parameter from the 12km simulations (61.2ms^{-1}). While the Bias Correction parameter estimates fall narrowly within the 95% confidence interval, both calibration pathways give similar predictions. This provides some reassurance in past results as downscaling estimates premised on a statistical distribution (e.g. Done et al. 2012; Pryor and Barthelmie 2013) have not distinguished between calibration pathways. It also emphasizes the importance of accounting for uncertainty in the future wind speed estimates by using both calibration pathways.

Shape parameter estimates are the same for each calibration pathway, as dictated by Equation 4, and are overestimated due to the large change in shape parameter between the control and future simulations that is not found in the 12km simulations. As no higher resolution future period simulations exist with these model runs, it is not possible to test the influence of model resolution on the relative changes in predicted tropical cyclones. Further, as simulation results are only available for 1995-2005, it is not possible to verify the methodology using a hindcast estimate of a different period of observations. These results suggest that a hybrid dynamical-statistical approach is required – using higher resolution (12km) grid simulations to allow tropical cyclone formation, followed by recalibration to achieve the appropriate range of maximum wind speeds.

4.3 Estimate of Future Wind Speeds

The parameter estimates were next used to derive the future distribution of maximum wind speeds, through the transformations in Equations 5-7, for 12km and 36km model simulations. Revised parameter estimates for the future distributions calculated from the bias correction and change factor calibration pathways are presented in Table 2. The recalibrated distribution parameters are compared with model and observed fitted distribution parameters in Figure 7.

Table 2 : Transformed parameter estimates for the future distribution of "observed" maximum wind speeds calculated from bias correction and change factor calibration methods

	Scale (α) ms^{-1}	Shape (β)
Bias Correction 36km Model	45.40	2.24
Change Factor 36km Model	40.34	2.24
Bias Correction 12km Model	42.56	2.06
Change Factor 12km Model	40.28	2.06

While the recalibrated scale parameters for each calibration pathway from the 36km simulations are close to the comparative 12km estimates, they have a wider range reflecting the difference in sample size between the observations and the simulations. It is likely that for both grid resolutions the bias correction pathway has overestimated the scale parameter, and underestimated it from the change factor pathway. The results are sufficiently close to suggest that this downscaling technique reduces some of the need for higher resolution simulations for maximum wind speed analyses, provided uncertainty is fully acknowledged. While the 36km recalibrated shape parameters are within an acceptable range for maximum wind speeds, the estimates do not fall within the same confidence interval as the observations. This is likely due to the large difference in shape parameters between the control and future simulations, and will lead to a lighter-tailed distribution and underestimates of the most extreme wind speeds. In contrast the 12km shape parameter estimates for the control and simulations are very close.

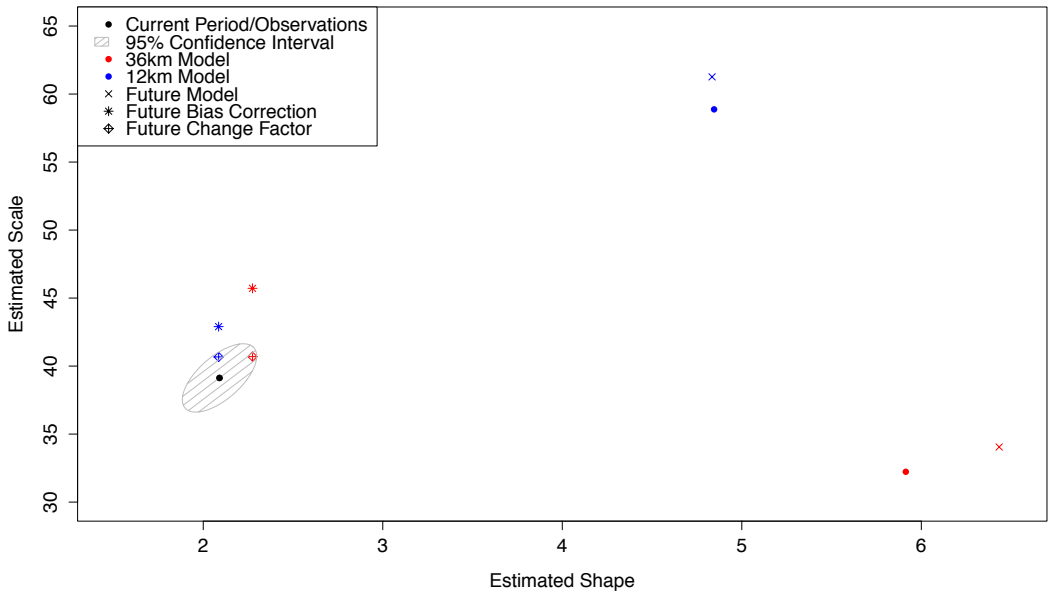

Figure 7 : Fitted and recalibrated left-truncated Weibull distribution parameters for the observations (black circle), 12km simulations (blue) and 36km simulations (red).

The different probability density functions (pdf) of the future wind speed obtained from the two recalibration pathways for 12km and 36km simulations are shown in Figure 8, and compared with the observations. The truncation threshold ($17ms^{-1}$) is indicated as a solid grey vertical line, below which the pdfs are faded out; Saffir-Simpson scales for hurricanes and winds thresholds (Simpson and Riehl 1981) are dot-dash vertical grey lines; 36km recalibrations are shown in red, 12km recalibrations are shown in blue, observations are in black; bias correction are shown with solid lines, change factor with dashed lines.

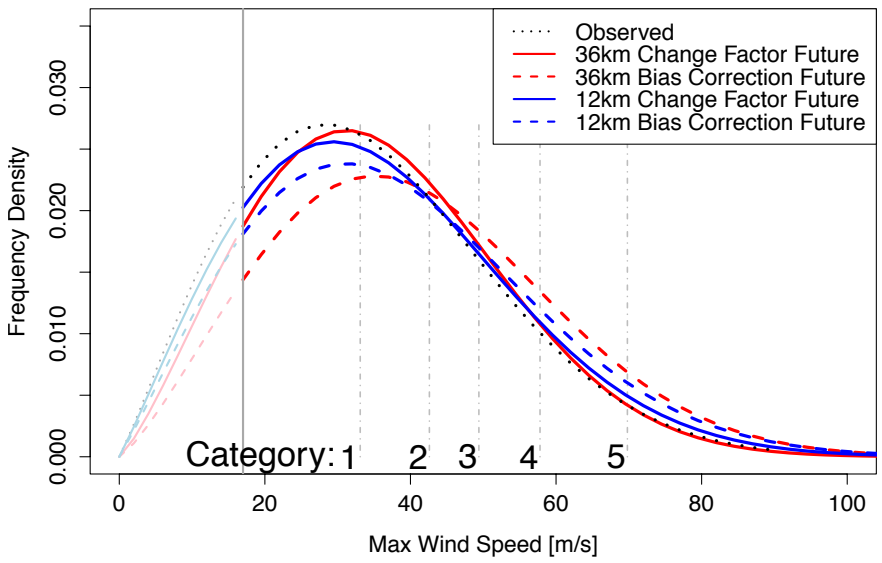

Figure 8 : Probability Density Functions for Bias Correction (solid lines) and Change Factor (dashed lines) transformations of future tropical cyclone maximum wind speeds for observations (black), 12km simulations (blue) and 36km simulations (red)

All recalibrated future projections of TC v_{max} indicate a decrease in the proportion of tropical storms (<30ms^{-1}) and increases in the proportion of the highest wind speeds (>50ms^{-1}). Bias correction re-parameterizations for both simulation resolutions indicate larger changes, both increases and decreases, in the proportions of tropical cyclones exceeding each of the Saffir-Simpson scale categories. Estimates of the proportion of TCs exceeding the three highest thresholds (49.4ms^{-1}, 57.8ms^{-1} and 69.8ms^{-1}) are shown in Table 3, comparing the observations for 1950-2010 and for 1995-2005 to the recalibrated wind speeds from 12km and 36km simulations for 2045-2055. 95% confidence intervals were estimated from 1000 bootstrap samples from left-truncated Weibull distributions with recalibrated shape and scale parameters.

Table 3 : Comparison of exceedance probabilities for Saffir-Simpson Category 3, 4 and 5 TCs using change factor or bias correction transformations to estimate future distribution parameters. Confidence Intervals in parentheses.

	>Category 3	>Category 4	>Category 5
Observations (1950-2010)	24.7% (±8.2%)	11.6% (±6.4%)	2.8 (±0.2%)
Observations (1995-2005)	21.3% (±7.2%)	9.1% (±5.6%)	1.6% (±0.4%)
Change Factor 36km (2045-2055)	26.5% (±8.0%)	12.3% (±6.7%)	2.8% (±0.5%)
Bias Correction 36km (2045-2055)	36.5% (±7.9%)	21.2% (±6.7%)	7.2% (±4.6%)
Change Factor 12km (2045-2055)	31.9% (±7.8%)	17.1% (±8.0%)	5.2% (±4.7%)
Bias Correction 12km (2045-2055)	36.8% (±7.6%)	23.3% (±6.3%)	9.8% (±4.0%)

While both recalibration pathways show increases in the proportion of wind speeds exceeding categories 3,4 and 5, the two methods give very different estimates of possible TC v_{max}. Increases are greatest between the bias corrected future estimates and current observations. Similarly, larger increases were obtained from the 12km simulations than from 36km simulations. However, the uncertainty arising from the recalibrated distributions is more substantial than differences between either model resolutions or different calibration pathways. There is insufficient evidence to select one calibration pathway in preference to the other; these results highlight the importance of using both calibration pathways to quantify the uncertainty in the likely range of future tropical cyclone maximum wind speeds.

5 Conclusion

The probability density function of model simulated tropical cyclone maximum wind speeds is much more peaked and less J-shaped than from that for observed maximum wind speeds. This study investigates probable explanations for the difference in distribution shape, concluding that model simulated wind speeds are more peaked (i.e. have a larger shape parameter) because the orthogonal velocity components are more constrained than Normally distributed variables and have lower variance. This arises from the low resolution of climate models with respect to the scale on which physical processes generate tropical cyclones in reality.

Weibull distributions provide a good fit to the observed and model simulated wind speeds. A powerful property of the Weibull distribution is that a simple power transform can be used to translate between two Weibull distributions with different parameters. Re-parameterizing the model wind speeds as a Weibull distribution, with shape parameter approaching 2 is a simple and effective method of transforming model wind speeds to more closely represent observations. This relationship leads to two distinct calibration pathways to estimate future projections of TC maximum wind speeds: bias correction and change factor.

The two calibration pathways give very similar estimates of the projected future wind speeds. Validation of the recalibration method using 12km simulated wind speeds as a proxy for "reality" indicates that neither calibration pathway is more accurate in estimating the changed scale parameter. The recalibrated scale parameters from the two calibration pathways encompasses the true scale parameter; both calibration methods are required to quantify the uncertainty in future estimates of tropical cyclone maximum

wind speeds. The recalibrated shape parameter is overestimated, likely due to the differences in shape parameter for the 36km control and future simulations, indicating that increases in the frequency of the highest wind speeds will be underestimated. As no higher resolution future period simulations exist with these model runs, it is not possible to test the influence of model resolution on the relative changes in predicted tropical cyclones here. However, other data sets (e.g. Bender et al. 2010) exist that also have low-resolution model results available which would permit sensitivity testing in the future.

Both calibration pathways indicate an increase in the proportion of tropical cyclones exceeding 49.4ms^{-1}; this increase is greater for the bias correction pathway and for 12km simulations. However, uncertainty in the estimates is greater than the differences between either the calibration pathways or model resolutions. Until one method can be demonstrated as more appropriate, it is important to present both sets of recalibration estimates to give a better representation of the uncertainty in future estimates (Katz et al. 2013).

Done et al. (2013) also found that the changes in TC v_{max} represented a shift in the distribution towards the right, with lower probability densities for Categories 1 and 2 storms. However, weather systems are limited by energy constraints that impose an upper limit to the maximum wind speed; this limit is changing at a slower rate than the overall distribution of wind speeds. As a result, not only is the distribution shifting toward the right, it is also transiting to a bimodal distribution of at the upper tail (Holland and Bruyère 2014). This additional feature is being investigated in an ongoing study. Furthermore, the recalibration approach assumes a single distribution for a given time period (e.g. 1950-2010 for the observations) with no temporal variability. Another

approach could allow the Weibull distribution parameters to shift over time, using a Generalized Linear Model.

An additional limitation lies in the probability that the model truncation will effect cyclones of different sizes differently. That is, a small cyclone will map to a much weaker intensity due to model truncation than a large one of the same intensity. The impact of this limitation on the approach presented here will require development of a data set of model results with resolution down to a few kilometers (e.g. Knutson et al. 2013).

Knutson et al. (2010) observed that some conflicting projections are due to model differences; however, the largest discrepancies arise between different downscaling approaches with decreases in maximum wind speeds more often reported from statistical-dynamical downscaling. Another explanation for differences in published estimates of future wind speeds is the nature of the statistical downscaling technique, e.g. using some form of linear modeling to incorporate sea surface temperature (SST) dependence (Elsner et al. 2008). Vecchi *et al.* (2008) found that it is unclear whether TC v_{max} are dependent on relative or absolute values of SST, though Bruyère et al (2012) noted no significant relative SST relationship once the in situ SST relationship was removed. Future projections show no change for relative SST (Knutson et al. 2010) but a substantial increase in intensity using in situ SST and potential intensity of SST (C. Bruyere, personal communication 2013).

The benefit of employing a parametric recalibration approach is the ability to increase the sample size beyond the limited scope of climate models output in a less computationally expensive manner (Done et al. 2013). This further allows some

estimation of the most extreme wind speeds that are physically possible but have not yet been observed. However, some caution must be applied in extrapolating the Weibull beyond the scope of observed wind speeds given the tendency to overestimate the most extreme wind speeds (Jagger et al. 2001). Extreme value distributions may improve the representation of these very high-tails by avoiding unrepresentative extrapolation, but further limiting the sample size to comply with extreme value distribution assumptions (Coles 2001) is a serious limitation where the data are already scarce and where the distribution may tend towards a bimodal shape (Holland and Bruyère 2014). Furthermore, any re-parameterization will be subject to the same conflict of two potentially opposing calibration pathways described here.

A possible alternative is to adopt a semi-parametric recalibration approach developed from the model representation of the orthogonal velocity components. Initial results presented in Section 3 indicated that the model shape parameter can be recalibrated close to the observed shape parameter by adding appropriate amounts of sub-grid scale Gaussian noise to the model orthogonal velocity components. That is, a simple Gaussian stochastic parameterization scheme on the wind speed components appears to rectify problems in the model-simulated wind speed and alleviate any further need for calibration. Work is progressing on this alternative recalibration method and to determine how the Gaussian noise variance depends on model grid resolution. If the sub-grid scale noise in the wind components is uncorrelated, the Gaussian noise will scale as the area of the model grid cell. Thus, a Gaussian process to represent the stochastic variation of unresolved sub grid-scale in the velocity components may present a more robust recalibration technique.

Acknowledgements

The National Center for Atmospheric Research is sponsored by the National Science Foundation (NSF); support for this work was provided by the Willis Research Network, the Research Program to Secure Energy for America and NSF EASM grant S1048841. We thank Sherrie Fredrick for extracting data, and Cindy Bruyère, James Done and Ben Youngman for productive discussions which enhanced this research.

Appendix 1: R Code for estimating left-truncated Weibull distribution parameters

```
# Left-truncated Weibull log likelihood function
ll.tweib <- function(pars, vec, u, n) {
     logalpha <- pars[1]
     logb <- pars[2]
     pars <- exp(pars)
     alpha <- pars[1]
     beta <- pars[2]
     l1 <- n * (logb - beta * logalpha)
     l2 <- (beta - 1) * sum(log(vec))
     l3 <- (alpha ^ (-beta)) * sum(vec ^ k)
     return( - l1 - l2 + l3 - n * (u / alpha) ^ beta)
}

# Function to fit left-truncated Weibull distribution
fit.tweib <- function(vec, trunc.pt, inits) {
     id.u <- vec > trunc.pt
     vec.u <- vec[id.u]
     out <- optim(log(inits), ll.tweib, vec = vec.u, u =
trunc.pt, n = sum(id.u))
     ests <- exp(out$par)
     names(ests) <- c("scale", "shape")
     return(ests)
}
```

```
# Function to invert left-truncated Weibull CDF
qweib <- function(x, lambda, k) lambda * (-log(1 - x)) ^ (1
/ k)


# Left-truncated Weibull density function
dtweib <- function(x, u, alpha, beta) {
     k * (alpha ^ (-beta)) * (x ^ (beta - 1)) *
          exp(- (x / alpha) ^ beta) * exp( (u / alpha) ^
beta)}
```

Appendix 2: Change Factor and Bias Correction parameter adjustments

Consider that wind speeds are distributed as a Weibull with $X \sim Wei(\alpha,\beta)$ and $x>0,\alpha>0,\beta>0$, then the cumulative distribution function and associated quantile function for p is:

$$F(x)=\Pr(X\le x)=1-\exp(-x/\alpha)^{\beta}=p$$
$$x=\alpha(-\ln(1-p))^{1/\beta}=F^{-1}(p)$$

$$F'(x)=\frac{dF}{dx}=\frac{\beta}{\alpha}\left(\frac{x}{\alpha}\right)^{(\beta-1)}e^{\left(-\frac{x}{\alpha}\right)^{\beta}}$$

Consider also that the transformation of $X \sim Wei(\alpha,\beta)$ has an exponential distribution Z, such that $Z=\left(\frac{X}{\alpha}\right)^{\beta} \sim Wei(1,1)=Exp(1)$ and $F(z)=1-e^{-Z}$.

Let X represent current climate observations, Y represents control climate model simulations, Y' represents future climate model simulations and X' are the unknown future climate observations.

All of the distributions are related through the Z transformation of *Wei(1,1)*, thus relationships can be derived to find the distribution of X' from X, Y and Y' through change factors (Y -> Y') or bias correction (X -> Y)

Change Factor

Assume a relationship between the future "observations", X', and future model simulations, Y', through the control simulations, Y, and transfer function Z.

$$X' = g(X)$$
$$Y' = g(Y)$$
$$Z = \left(\frac{Y}{\alpha_Y}\right)^{\beta_Y}$$
$$Y' = \alpha_{Y'} Z^{1/\beta_{Y'}} = \alpha_{Y'}\left(\frac{Y}{\alpha_Y}\right)^{\beta_Y/\beta_{Y'}}$$
$$\therefore X' = \alpha_{Y'}\left(\frac{X}{\alpha_Y}\right)^{\beta_Y/\beta_{Y'}} = \alpha_{Y'}\left(\frac{\alpha_X Z^{1/\beta_X}}{\alpha_Y}\right)^{\beta_Y/\beta_{Y'}}$$
$$= \alpha_{Y'}\left(\frac{\alpha_X}{\alpha_Y}\right)^{\beta_Y/\beta_{Y'}} Z^{\beta_Y/\beta_X\beta_{Y'}}$$
$$= \left(\frac{Z}{\left(\frac{1}{\alpha_{Y'}}\left(\frac{\alpha_Y}{\alpha_X}\right)^{\beta_Y/\beta_{Y'}}\right)^{\beta_X\beta_{Y'}/\beta_Y}}\right)^{\beta_Y/\beta_X\beta_{Y'}} = \left(\frac{Z}{\alpha_{X'}}\right)^{1/\beta_{X'}}$$

Then using the Z transform $X = \alpha Z^{1/\beta}$ and rearranging, expressions for the scale and shape are derived as:

$$\beta_{X'} = \frac{\beta_X \beta_{Y'}}{\beta_Y}$$

$$\alpha_{X'} = \alpha_{Y'} \left(\frac{\alpha_X}{\alpha_Y} \right)^{\beta_Y / \beta_{Y'}}$$

Bias Correction

Assume a relationship between the current observations, *X*, and the future "observations", *X*' through the transfer function for the control simulation, *Y*, whereby:

$$X = g(Y) \quad \text{and} \quad Z = \left(\frac{Y}{\alpha_Y} \right)^{\beta_Y}$$

$$X' = g(Y') \quad \text{and} \quad Z = \left(\frac{X}{\alpha_X} \right)^{\beta_X}$$

then

$$X = \alpha_X Z^{1/\beta_X} = \alpha_X \left(\frac{Y}{\alpha_Y} \right)^{\beta_Y / \beta_X}$$

$$X' = \alpha_X \left(\frac{Y'}{\alpha_Y} \right)^{\beta_Y / \beta_X}$$

$$Y' = \alpha_{Y'} Z^{1/\beta_{Y'}}$$

and so it follows that

$$X' = \alpha_X \left(\frac{\alpha_{Y'} Z^{1/\beta_{Y'}}}{\alpha_Y} \right)^{\beta_Y / \beta_X}$$

$$= \left(\frac{Z}{\frac{1}{\alpha_X \frac{\beta_X \beta_{Y'}}{\beta_Y}} \left(\frac{\alpha_Y}{\alpha_{Y'}} \right)^{\beta_{Y'}}} \right)^{\beta_Y / \beta_X \beta_{Y'}}$$

and then the expressions for shape and scale can be derived as before, with the same relationship for shape as for Change Factor.

$$\beta_{X'} = \frac{\beta_X \beta_{Y'}}{\beta_Y}$$

$$\alpha_{X'} = \alpha_X \left(\frac{\alpha_{Y'}}{\alpha_Y} \right)^{\beta_Y / \beta_X}$$

6 Bibliography

Batts, M. E., E. Simiu, and L. R. Russell, 1980: Hurricane Wind Speeds in the United States. *J. Struct. Div.*, **106**, 2001–2016.

Bender, M. A., T. R. Knutson, R. E. Tuleya, J. J. Sirutis, G. A. Vecchi, S. T. Garner, and I. M. Held, 2010: Modeled impact of anthropogenic warming on the frequency of intense Atlantic hurricanes. *Science*, **327**, 454–458, doi:10.1126/science.1180568.

Benton, T., B. Gallani, C. Jones, K. Lewis, and R. Tiffin, 2012: *Severe weather and UK food chain resilience Detailed Appendix to Synthesis Report*. London, UK,.

Brown, C., and R. L. Wilby, 2012: An Alternate Approach to Assessing Climate Risks. *Eos Trans. Am. Geophys. Union*, **92**, 92–94.

Bruyère, C. L., G. J. Holland, and E. Towler, 2012: Investigating the Use of a Genesis Potential Index for Tropical Cyclones in the North Atlantic Basin. *J. Clim.*, **25**, 8611–8626, doi:10.1175/JCLI-D-11-00619.1.

Bürger, G., T. Q. Murdock, a. T. Werner, S. R. Sobie, and a. J. Cannon, 2012: Downscaling Extremes—An Intercomparison of Multiple Statistical Methods for Present Climate. *J. Clim.*, **25**, 4366–4388, doi:10.1175/JCLI-D-11-00408.1.

Coles, S., 2001: *An Introduction to Statistical Modeling of Extreme Values*. Springer-Verlag, Berlin,.

Collins, W. D. and Coauthors, 2006: The Community Climate System Model Version 3 (CCSM3). *J. Clim.*, **19**, 2122–2143, doi:10.1175/JCLI3761.1.

Conradsen, K., L. B. Nielsen, and L. P. Prahm, 1984: Review of Weibull Statistics for Estimation of Wind Speed Distributions. *J. Clim. Appl. Meteorol.*, **23**, 1173–1183, doi:10.1175/1520-0450(1984)023.

Curry, C. L., D. van der Kamp, and A. H. Monahan, 2011: Statistical downscaling of historical monthly mean winds over a coastal region of complex terrain. I. Predicting wind speed. *Clim. Dyn.*, **38**, 1281–1299, doi:10.1007/s00382-011-1173-3.

Davis, C. and Coauthors, 2008: Prediction of Landfalling Hurricanes with the Advanced Hurricane WRF Model. *Mon. Weather Rev.*, **136**, 1990–2005, doi:10.1175/2007MWR2085.1.

Done, J. M., G. J. Holland, C. L. Bruyère, R. Leung, and A. Suzuki-Parker, 2012: *Modeling high-impact weather and climate: Lessons from a tropical cyclone perspective. NCAR Technical Note NCAR/TN-490+STR*. Boulder, CO,.

Done, J. M., G. J. Holland, C. L. Bruyère, L. R. Leung, and A. Suzuki-Parker, 2013: Modeling high-impact weather and climate: lessons from a tropical cyclone perspective. *Clim. Change*, doi:10.1007/s10584-013-0954-6.

Elsner, J. B., J. P. Kossin, and T. H. Jagger, 2008: The increasing intensity of the strongest tropical cyclones. *Nature*, **455**, 92–95, doi:10.1038/nature07234.

Emanuel, K., 2006: Climate and Tropical Cyclone Activity: A New Model Downscaling Approach. *J. Clim.*, **19**, 4797–4802, doi:10.1175/JCLI3908.1.

Executive Office of the President, 2013: *The President's Climate Action Plan*. Washington D.C., USA,.

Heckert, N. A., E. Simiu, and T. Whalen, 1998: Estimates of hurricane wind speeds by "Peaks over threshold" method. *J. Struct. Eng.*, **124**, doi:0733-9445/98/0004-0045-0049.

Ho, C. K., D. B. Stephenson, M. Collins, C. a. T. Ferro, and S. J. Brown, 2012: Calibration Strategies: A Source of Additional Uncertainty in Climate Change Projections. *Bull. Am. Meteorol. Soc.*, **93**, 21–26, doi:10.1175/2011BAMS3110.1.

Holland, G., and C. L. Bruyère, 2014: Recent intense hurricane response to global climate change. *Clim. Dyn.*, doi:10.1007/s00382-013-1713-0.

Holland, G. J., 2008: A Revised Hurricane Pressure-Wind Model. *Mon. Weather Rev.*, **136**, 3432–3445.

IPCC, 2013: *IPCC WG1 Contribution to the Fifth Assessment Report. Climate Change 2013: The Physical Science Basis. Summary for Policy Makers*. Geneva, Switzerland,.

IPCC SRES SPM, 2000: *Summary for policymakers, emissions scenarios: a special report of IPCCWorking Group III*. Geneva, Switzerland,.

Jagger, T., J. B. Elsner, and X. Niu, 2001: A Dynamic Probability Model of Hurricane Winds in Coastal Counties of the United States. *J. Appl. Meteorol.*, **40**, 853–863, doi:10.1175/1520-0450(2001)040.

Justus, C. G., W. R. Hargraves, A. Mikhail, and D. Graber, 1978: Methods for Estimating Wind Speed Frequency Distributions. *J. Appl. Meteorol.*, **17**, 350–353, doi:10.1175/1520-0450(1978)017.

Kallache, M., M. Vrac, P. Naveau, and P. Michelangeli, 2011: Nonstationary probabilistic downscaling of extreme precipitation. *J. Geophys. Res.*, **116**, 1–15, doi:10.1029/2010JD014892.

Van der Kamp, D., C. L. Curry, and A. H. Monahan, 2011: Statistical downscaling of historical monthly mean winds over a coastal region of complex terrain. II. Predicting wind components. *Clim. Dyn.*, **38**, 1301–1311, doi:10.1007/s00382-011-1175-1.

Katz, R. W., P. F. Craigmile, P. Guttorp, M. Haran, B. Sansó, and M. L. Stein, 2013: Uncertainty analysis in climate change assessments. *Nat. Clim. Chang.*, **3**, 769–771, doi:10.1038/nclimate1980.

Knapp, K. R., M. C. Kruk, D. H. Levinson, H. J. Diamond, and C. J. Neumann, 2010: The International Best Track Archive for Climate Stewardship (IBTrACS). *Bull. Am. Meteorol. Soc.*, **91**, 363–376.

Knutson, T. R. and Coauthors, 2010: Tropical cyclones and climate change. *Nat. Geosci.*, **3**, 157–163, doi:10.1038/ngeo779.

Knutson, T. R. and Coauthors, 2013: Dynamical Downscaling Projections of Twenty-First-Century Atlantic Hurricane Activity: CMIP3 and CMIP5 Model-Based Scenarios. *J. Clim.*, **26**, 6591–6617, doi:10.1175/JCLI-D-12-00539.1.

Knutti, R., D. Masson, and A. Gettelman, 2013: Climate model genealogy: Generation CMIP5 and how we got there. *Geophys. Res. Lett.*, **40**, doi:10.1002/grl.50256.

Kossin, J. P., K. R. Knapp, D. J. Vimont, R. J. Murnane, and B. A. Harper, 2007: A globally consistent reanalysis of hurricane variability and trends. *Geophys. Res. Lett.*, **34**, L04815, doi:10.1029/2006GL028836.

Lafon, T., S. Dadson, G. Buys, and C. Prudhomme, 2013: Bias correction of daily precipitation simulated by a regional climate model: a comparison of methods. *Int. J. Climatol.*, **33**, 1367–1381, doi:10.1002/joc.3518.

Maraun, D. and Coauthors, 2010: Precipitation downscaling under climate change: Recent developments to bridge the gap between dynamical models and the end user. *Rev. Geophys.*, **48**, RG3003, doi:10.1029/2009RG000314.

Monahan, A. H., 2011: Can We See the Wind? Statistical Downscaling of Historical Sea Surface Winds in the Subarctic Northeast Pacific. *J. Clim.*, **25**, 1511–1528, doi:10.1175/2011JCLI4089.1.

Monahan, A. H., 2013: The Gaussian Statistical Predictability of Wind Speeds. *J. Clim.*, **26**, 5563–5577, doi:10.1175/JCLI-D-12-00424.1.

Murphy, J. and Coauthors, 2009: *Climate change projections*. Met Office Hadley Centre, Exeter ET - July 2nd 2009,.

Piani, C., J. O. Haerter, and E. Coppola, 2009: Statistical bias correction for daily precipitation in regional climate models over Europe. *Theor. Appl. Climatol.*, **99**, 187–192, doi:10.1007/s00704-009-0134-9.

Pryor, S. C., 2005: Empirical downscaling of wind speed probability distributions. *J. Geophys. Res.*, **110**, D19109, doi:10.1029/2005JD005899.

Pryor, S. C., and R. J. Barthelmie, 2013: Assessing the vulnerability of wind energy to climate change and extreme events. *Clim. Change*, doi:10.1007/s10584-013-0889-y.

Rummukainen, M., 2010: State-of-the-art with regional climate models. *WIREs Clim. Chang.*, **1**, 82–96, doi:10.1002/wcc,8.

Salameh, T., P. Drobinski, M. Vrac, and P. Naveau, 2008: Statistical downscaling of near-surface wind over complex terrain in southern France. *Meteorol. Atmos. Phys.*, **103**, 253–265, doi:10.1007/s00703-008-0330-7.

Simpson, R. H., and H. Riehl, 1981: *The Hurricane and Its Impact*. John Wiley & Sons, Incorporated,.

Skamarock, W., J. B. Klemp, J. Dudhia, D. O. Gill, D. Barker, M. G. Duda, X. Huang, and W. Wang, 2008: *A Description of the Advanced Research WRF Version 3. NCAR Technical Note NCAR/TN-475+STR*. Boulder, CO,.

Stewart, D. A., and O. M. Essenwanger, 1978: Frequency Distribution of Wind Speed Near the Surface. *J. Appl. Meteorol.*, **17**, 1633–1642, doi:10.1175/1520-0450(1978)017.

Suzuki-Parker, A., 2012: Uncertainties and Limitations in Simulating Tropical Cyclones.

Tuller, S. E., and A. C. Brett, 1985: The goodness of fit of the weibull and rayleigh distributions to the distributions of observed wind speeds in a topographically diverse area. *J. Climatol.*, **5**, 79–94, doi:10.1002/joc.3370050107.

Vecchi, G. A., K. L. Swanson, and B. J. Soden, 2008: Climate change. Whither hurricane activity? *Science*, **322**, 687–689, doi:10.1126/science.1164396.

Whetton, P., K. Hennessy, J. Clarke, K. McInnes, and D. Kent, 2012: Use of Representative Climate Futures in impact and adaptation assessment. *Clim. Change*, **115**, 433–442, doi:10.1007/s10584-012-0471-z.

Wilks, D. S., 2011: *Statistical methods in the atmospheric sciences*. 3rd ed. Academic Press Inc., Waltham, MA,.

Zhou, Y., and S. J. Smith, 2013: Spatial and temporal patterns of global onshore wind speed distribution. *Environ. Res. Lett.*, **8**, 034029, doi:10.1088/1748-9326/8/3/034029.